PRIMEVAL ADIABATIC PERTURBATION
IN AN EXPANDING UNIVERSE*

P. J. E. PEEBLES†
Joseph Henry Laboratories, Princeton University

AND

J. T. YU‡
Goddard Institute for Space Studies, NASA, New York
Received 1970 January 5; revised 1970 April 1

ABSTRACT

The general qualitative behavior of linear, first-order density perturbations in a Friedmann-Lemaître cosmological model with radiation and matter has been known for some time in the various limiting situations. An exact quantitative calculation which traces the entire history of the density fluctuations is lacking because the usual approximations of a very short photon mean free path before plasma recombination, and a very long mean free path after, are inadequate. We present here results of the direct integration of the collision equation of the photon distribution function, which enable us to treat in detail the complicated regime of plasma recombination. Starting from an assumed initial power spectrum well before recombination, we obtain a final spectrum of density perturbations after recombination. The calculations are carried out for several general-relativity models and one scalar-tensor model. One can identify two characteristic masses in the final power spectrum: one is the mass within the Hubble radius ct at recombination, and the other results from the linear dissipation of the perturbations prior to recombination. Conceivably the first of these numbers is associated with the great rich clusters of galaxies, the second with the large galaxies. We compute also the expected residual irregularity in the radiation from the primeval fireball. If we assume that (1) the rich clusters formed from an initially adiabatic perturbation and (2) the fireball radiation has not been seriously perturbed after the epoch of recombination of the primeval plasma, then with an angular resolution of 1 minute of arc the rms fluctuation in antenna temperature should be at least $\delta T/T = 0.00015$.

I. INTRODUCTION

a) Purpose

The possible discovery of radiation from the primeval fireball opens a promising lead toward a theory of the origin of galaxies. This primeval radiation would serve, first, to fix an epoch at which nonrelativistic bound systems like galaxies can start to develop (Peebles 1965a), and second, to impress on the power spectrum of initial density fluctuations characteristic lengths and masses (Gamow 1948; Peebles 1965a, 1967a; Michie 1967; Silk 1968). These characteristic features in the power spectrum hopefully result from all the complicated details of the evolution of the Universe *after* the initial power spectrum is arbitrarily set at some very early epoch. If one can make a reasonable argument for a coincidence of these features with observed phenomena, it will provide an important encouragement and guide to the further development of the theory. A more direct observational test of these processes might be provided by the residual small-scale fluctuations in the microwave background (Peebles 1965b; Sachs and Wolfe 1967; Silk 1968; Wolfe 1969; Longair and Sunyaev 1969), if we assume that this radiation has not been further scattered (Dautcourt 1969).

According to Zel'dovich (1967) there are two kinds of perturbations that are of interest: initial isothermal perturbations and initially adiabatic perturbations. It has been suggested that the globular clusters are the remnants of an isothermal perturbation in the early Universe (Peebles and Dicke 1968; Peebles 1969). Our purpose here is to discuss in some detail the evolution of adiabatic density fluctuations in the primeval-fireball picture.

An initially adiabatic perturbation evolves through four regimes: (a) When the age t of the Universe is much less than λ/c, where λ is the characteristic scale of the perturbation, a fractional perturbation $\delta\rho/\rho$ to the total mass density grows with time, but the entropy per nucleon is conserved (hence adiabatic). (b) When $\lambda \ll ct$, the perturbation oscillates like an acoustic wave. (c) As the Universe expands through the recombination phase, the photon mean free path becomes comparable to λ, and the oscillating wave is attenuated, leaving some residual perturbation in the matter distribution. (d) When $T \lesssim 2500°$ K, recombination is sufficiently complete that radiation drag on the matter may be neglected, and the residual perturbation may start to grow into bound systems like protogalaxies.

The above general scheme for initially adiabatic perturbations was already given by Lifshitz (1946). The very complicated regime (c) has been considered by a number of people in a variety of approximations, with the general conclusion that initially adiabatic perturbations on a characteristic mass scale $\lesssim 10^{11}$–10^{13} $\mathfrak{M}_\odot$ are strongly attenuated. This problem was first considered in approximations to first order in the photon mean free time t_c independently by Michie (1967), Peebles (1967a), and Silk (1968). It has since been considered by Bardeen (1968) in the first twenty moments of the radiation distribution function, and by Field (1970a), who solves the problem to all orders in t_c when the expansion of the Universe may be neglected. However, these approximation schemes run afoul of the enormous variation and rate of variation of the photon mean free path through the epoch of recombination. As a result, previous workers on this subject (Peebles 1967a; Michie 1967; Silk 1968; Field and Shepley 1968) could give only qualitative estimates of the different characteristic masses involved here. To obtain a more accurate description of the evolution through this complicated phase of recombination, we have resorted to direct numerical integration of the collision equation for the photon distribution function.

The more quantitative results of the present calculation are compared with the earlier estimates in § VII. We also discuss there the possible significance of these results. In § II we derive the differential equations to be integrated. It is impractical to integrate the collision equation numerically in the very early Universe because the photon mean free path t_c is so short, but here it becomes a good approximation to describe the radiation as a fluid with viscosity. This description of the radiation was used in all the previous work (Lifshitz 1946; Michie 1967; Silk 1968; Field and Shepley 1968), and is indeed a good approximation in this early epoch. The fluid description of radiation is equivalent to an expansion and integration of our collision equation to first order in t_c. In § III we give the resulting equations valid to first order in t_c, and we present solutions to these approximate equations under various limiting conditions. These results are used to start the numerical integration and to check numerical accuracy. In § IV we consider the residual perturbation to the microwave background. The numerical integrations are described in §§ V and VI.

b) Assumptions and Approximations

In the following calculations we use either conventional general-relativity theory, with cosmological constant Λ equal to zero, or the scalar-tensor theory (Brans and Dicke 1961). We start from a homogeneous, isotropic cosmological model, in which the present parameters are

$$H_0^{-1} = 1 \times 10^{10} \text{ years}, \quad T_0 = 2.7° \text{ K}. \tag{1}$$

We consider four cosmological models: (*a*) an open general-relativity model with present mass density $\rho_0 = 0.03\rho_c$, where ρ_c is the present density in the cosmologically flat general-relativity model; (*b*) the cosmologically flat general-relativity model; (*c*) a closed general-relativity model, $\rho_0 = 5\rho_c$; and (*d*) a cosmologically flat scalar-tensor model with coupling constant $\omega = 5$.

As pointed out by Sachs and Wolfe (1967), it is very convenient to assume that the metric for the unperturbed cosmological model satisfies the approximate formula

$$ds^2 = dt^2 - a(t)^2[(dx^1)^2 + (dx^2)^2 + (dx^3)^2] . \tag{2}$$

To justify this approximation we note that the present cosmological parameters satisfy

$$H_0^2 = \tfrac{8}{3}\pi G\rho_0 \pm \frac{c^2}{R^2 a_0^2} . \tag{3}$$

In the models we consider $\rho_0 \geq 0.03\rho_c$, so by equation (3)

$$\tfrac{8}{3}\pi G\rho_0 \gtrsim \frac{0.03c^2}{R^2 a_0^2} . \tag{4}$$

Therefore, at the epoch of recombination (redshift $Z \sim 1000$) we have

$$\tfrac{8}{3}\pi G\rho_r \gtrsim \frac{30c^2}{R^2 a_r^2} . \tag{5}$$

We are interested in perturbations with characteristic length $l = a_r r$ less than or comparable to the Hubble length at recombination,

$$a_r r \lesssim \frac{c}{(8\pi G\rho_r/3)^{1/2}} \lesssim a_r R/(30)^{1/2} , \tag{6}$$

where the second inequality follows from equation (5). Equation (6) shows that in cosmological models of interest it is a reasonable approximation to neglect $(r/R)^2$ compared with unity, as we have done in the line element (2). A similar argument applies to the closed model.

In the general-relativity cosmologies we use the connection between time and density given by Peebles (1968). For the scalar-tensor cosmology we express the scalar field $\phi_0(t)$ for the unperturbed model as

$$\phi_0 = \frac{4 + 2\omega}{3 + 2\omega}\frac{\lambda(t)}{G_0} , \tag{7}$$

where G_0 is Newton's constant, and $\lambda(t)$ has a present value of unity. The equations governing the rate of expansion of the model are

$$\left(\frac{1}{a}\frac{da}{dt} + \frac{1}{2\lambda}\frac{d\lambda}{dt}\right)^2 = \frac{8\pi G_0(3 + 2\omega)}{3\lambda(4 + 2\omega)}(\mathcal{E} + \rho) + \tfrac{1}{4}\left(1 + \frac{2\omega}{3}\right)\frac{1}{\lambda^2}\left(\frac{d\lambda}{dt}\right)^2 , \tag{8a}$$

$$\frac{d\lambda}{dt} = \frac{8\pi G_0\rho t}{4 + 2\omega} , \tag{8b}$$

where ρ and $\mathcal{E}$ are the mass densities of matter and radiation. Equation (8b) is the result of a first integration of the field equation for ϕ, and we have set the constant of integration equal to zero. This corresponds to Dicke's solution of type 1 (Dicke 1968, Fig. 4). Equations (8) are integrated numerically to fit the boundary values $\lambda = 1$ and $(da/dt)/a = H_0$ now.

For simplicity we assume that the matter is pure hydrogen. We describe the matter as an ideal fluid with zero pressure and zero heat capacity. The heat capacity of the radiation is in fact some eight orders of magnitude larger than that of matter. The matter pressure defines a characteristic Jeans mass $\mathfrak{M} \sim 10^5 \, \mathfrak{M}_\odot$. In the present paper we consider dimensions much larger than this, so the matter pressure is negligible. A measure of the relative importance of the off-diagonal terms in the stress tensors for the matter and radiation is given by the ratio of shear viscosities of matter and radiation,

$$\eta_p/\eta_\gamma \sim (l_p/l_\gamma)(\rho_p/\rho_\gamma)\bar{v}_p/c \sim 10^{-19}(T/T_0)^{3/2} \ . \qquad (9)$$

Here the subscript p refers to the protons, the mean free path l_γ for the radiation is fixed by Thomson scattering by the free electrons, and the mean free path l_p for the protons is fixed by Coulomb scattering in the plasma. We conclude from equation (9) that the momentum transfer by the matter is negligible at all epochs of interest $(T \lesssim 10^{10} \, ^\circ\mathrm{K})$. It might be mentioned finally that for the irrotational perturbations considered here the polarization field keeps the electrons and protons moving together to high accuracy.
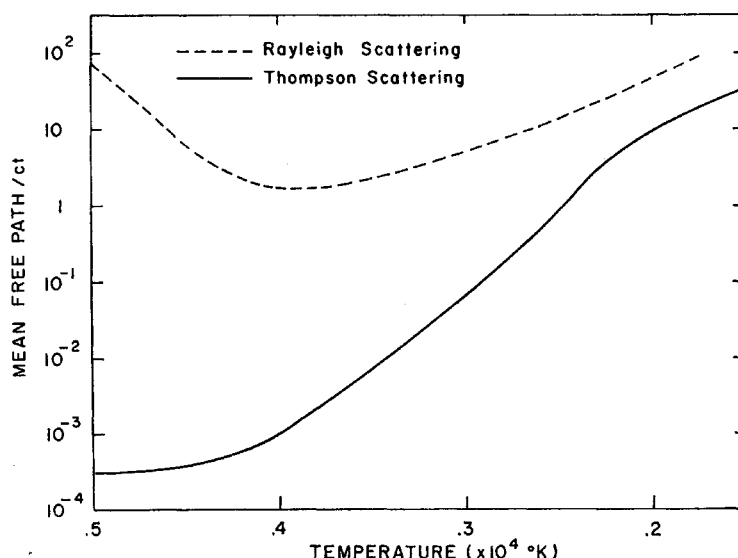

FIG. 1.—Mean free paths for Thomson scattering and Rayleigh scattering in the flat general-relativity model.

The radiation will be described by a distribution function f. In the numerical computation of f an important parameter is the mean free path for scattering the radiation. The most important process here is Thomson scattering by the free electrons; the next most important, Rayleigh scattering by atomic hydrogen. In Figure 1 we plot the mean free paths for these two processes. For Thomson scattering

$$l_\mathrm{T} = (\sigma n_e)^{-1} \ , \qquad (10)$$

where n_e is the electron density. We obtain an average cross-section for Rayleigh scattering by integrating over the blackbody distribution,

$$\langle\sigma_\mathrm{R}\rangle = \int \sigma_\mathrm{R}(\nu)i_\nu d\nu / \int i_\nu d\nu \ ,$$

and we set

$$l_\mathrm{R} = (n_\mathrm{H}\langle\sigma_\mathrm{R}\rangle)^{-1} \ , \qquad (11)$$

where n_H is the number density of hydrogen atoms. In the computation of the mean free path we use the approximate theory of plasma recombination in the primeval fireball as given by Peebles (1968), assuming zero primeval helium.

As shown in the figure, the ratio of mean free paths for Rayleigh and Thomson scattering reaches a minimum value of ~ 5 near the end of the epoch of recombination, when the mean free path for Thomson scattering is a factor of 10 larger than the Hubble radius. These results are based on the cosmologically flat model. If ρ_0 were smaller, the ratio of Rayleigh to Thomson mean free paths would be increased (because the residual ionization would be higher).

The next important process is free-free bremsstrahlung emission from the plasma. A direct calculation, using Kramers' approximate formula, gives the ratio of mean free path to Hubble radius just prior to recombination as

$$\frac{l_{ff}}{ct} \sim 10^5 \ .$$

The production of molecular hydrogen is found to be less than about one part in 10^5, and these molecules have negligible effect on the radiation.

We conclude that it is a reasonable approximation to take account of Thomson scattering only. The error in neglecting Rayleigh scattering only becomes appreciable (~ 20 percent of Thomson) once the Universe is already transparent.

To simplify the computation further, we introduce the additional approximation that Thomson scattering is isotropic (instead of varying as $\cos^2 \theta$) in the matter rest frame.

A basic assumption in all this discussion is that the very early Universe is only slightly perturbed away from the thermodynamic-equilibrium, homogeneous, and isotropic state. This means in particular that there is not supposed to be a primeval magnetic field. The picture breaks down once the earliest bound systems form. If this happens after the initial decoupling of matter and radiation is complete, it will not affect the computation of the density-perturbation transfer function. It is a separate and quite uncertain problem whether subsequent processes could scatter and smooth out the fireball radiation.

For initial values, it seems reasonable to assume that the perturbation is confined almost entirely to the most rapidly growing mode (Peebles 1967b). This is because it would be surprising to find at any epoch that the amplitude of the most rapidly growing mode was very much smaller than any of the others, for this would require a highly special perturbing influence. If we rule out this possibility at some very early epoch, it follows that at later epochs the most rapidly growing mode ought to be the dominant one. With this assumption the phase of the acoustic wave in the regime (b) mentioned above is fixed.

We consider separately two cases, (1) perturbation wavelength comparable to ct at recombination, and (2) wavelength much less than this characteristic value. In the first case, the transition between the regimes (a) and (b) mentioned above is of interest because it happens close to the recombination regime (c). In the second case, the transition from (a) to (b) has no interesting effect. Also, the perturbation here suffers a large number of oscillations prior to recombination, which makes it difficult to integrate the equations numerically and may make it unlikely that the phase predicted in the simple linear theory is preserved. Therefore in case (2) we simply start the integration in the regime (b), and we suppose here that the phase of each mode is chosen at random.

It might be argued on general grounds that our approach to the second case is the most reasonable one. As we attempt to trace the history of the Universe ever further back in time, our extrapolation surely is becoming more and more uncertain. Here we abandon all attempts to trace the expansion back earlier than $T \sim 10000°$ K, say, and we assume that at that epoch the adiabatic perturbation looks more or less like white noise.

The primeval neutrino density perturbation follows the matter and radiation through regime (a), and at the end of this regime the neutrino perturbation disperses because the mean free path is so long. As best we can see, this extra complication has no significant effect, so in our case (1) we ignore neutrinos altogether. In our case (2) the neutrinos

simply increase slightly the rate of expansion of the unperturbed cosmological model, and we have included this effect.

Throughout this paper Greek indices $\alpha, \beta, \ldots$, have a range from 1 to 3, and Latin indices from 0 to 3. Units are chosen such that the velocity of light is unity. We choose time-orthogonal coordinates so that the components of the metric tensor are

$$g_{00} = 1, \quad g_{0\alpha} = 0, \quad g_{\alpha\beta} = -a(t)^2[\delta_{\alpha\beta} - h_{\alpha\beta}(x, t)]. \tag{12}$$

In the scalar-tensor cosmology we write the scalar field as

$$\phi = \phi_0(t)[1 + \psi(x, t)], \tag{13}$$

where ϕ_0 is given by equation (7).

<center>II. THEORY</center>

<center>a) <i>Description of the Radiation</i></center>

Relativistic transport theory has been discussed by a number of authors (e.g., Lindquist 1966). For our purposes the most convenient approach seems to be the following. We start with a photon-gas picture, which is the limit as $m \rightarrow 0$ of the motion of a gas of particles of mass m. It will be recalled that when $m \neq 0$ the equations of motion of a particle may be derived from the action principle

$$\delta \int \mathcal{L} dt = 0, \quad \mathcal{L} = m(g_{ij}v^iv^j)^{1/2}, \quad v^i = \frac{dx^i}{dt}, \tag{14}$$

where $dt = dx^0$ is coordinate time. It follows that the momenta canonically conjugate to the coordinates x^α are

$$p_\alpha = \frac{\partial \mathcal{L}}{\partial v^\alpha} = mu_\alpha. \tag{15}$$

With these momenta the geodesic equations of motion are

$$\frac{dp_i}{dt} = \tfrac{1}{2}g_{jk,i}p^jv^k, \quad v^i = p^i/p^0, \tag{16}$$

where v^i is the coordinate velocity. Equations (16) remain well defined in the limit $m \rightarrow 0$, with

$$g_{ij}p^ip^j = 0. \tag{17}$$

We use equations (16) and (17) to describe the motion of the radiation.

The radiation distribution function is defined to be the number of photons per unit volume in configuration and momentum space,

$$dN = f(x, p)dx^1dx^2dx^3dp_1dp_2dp_3. \tag{18}$$

Since x^α and p_α are canonical coordinates, we know from Liouville's theorem that f is constant along the path of a particle. Since this is true whatever the choice of coordinates, f must be invariant against coordinate transformations.

<center>b) <i>Stress-Energy Tensor for the Radiation</i></center>

For an observer at rest in our chosen time-orthogonal coordinate system, the photon energy is just p_0, and the observed bolometric radiation brightness per steradian is

$$\int f p_0{}^3 dp_0 \equiv \mathcal{E}(t)[1 + \delta(\theta, \phi)]/4\pi. \tag{19}$$

Here $\mathcal{E}(t)$ is the radiation density in the unperturbed cosmological model, and δ is the fractional perturbation to the brightness. We represent the spatial components of the photon four-momentum in our coordinate frame in terms of the usual direction cosines γ_α,

$$p_\alpha = -p_0 a(t)e\gamma_\alpha, \tag{20}$$

where e is chosen to satisfy equation (17). In terms of these variables the components of the energy-momentum tensor are, to first order,

$$(T_r)_{00} = \mathcal{E}(1 + \delta_r) , \qquad \delta_r = \int \delta d\Omega/4\pi , \tag{21a}$$

$$(T_r)_{0a} = -a\mathcal{E}f_a , \qquad f_a = \int \delta\gamma_a d\Omega/4\pi , \tag{21b}$$

$$(T_r)_{a\beta} = a^2\mathcal{E}(\delta_{a\beta}/3 - h_{a\beta}/3 + \eta_{a\beta}) , \qquad \eta_{a\beta} = \int \delta\gamma_a\gamma_\beta d\Omega/4\pi . \tag{21c}$$

One can obtain these expressions by direct computation from the covariant expression for the energy-momentum tensor, or one can simply recognize that equations (21) follow by coordinate transformation from the usual special-relativistic expressions in locally Minkowski coordinates.

c) Collision Equation for the Radiation

We describe the radiation by the coordinate position and time (x^a, t), the direction cosines γ_a, and the photon energy p_0 (all in the time-orthogonal coordinate system). Then the collision equation for the distribution function becomes

$$\frac{\partial f}{\partial t} + \frac{\partial f}{\partial x^a}\frac{dx^a}{dt} + \frac{\partial f}{\partial\gamma_a}\frac{d\gamma_a}{dt} + \frac{\partial f}{\partial p_0}\frac{dp_0}{dt} = \sigma n_e \frac{p'_0}{p_0}(f_+ - f) . \tag{22}$$

Here n_e is the number density of free electrons observed in the matter rest frame, f_+ is the distribution function for the scattered radiation, and p'_0/p_0 is the correction for coordinate time from proper time in the matter rest frame. To first order,

$$p'_0/p_0 = 1 - v^a\gamma_a , \tag{23}$$

where v^a is the proper matter velocity relative to our coordinate frame.

Because f and f_+ differ by terms of first order in the perturbation, we can set $p'_0/p_0 = 1$ in the right-hand side of equation (22). In the third term on the left side of equation (22) $\partial f/\partial\gamma_a$ and $d\gamma_a/dt$ both are of first order in the perturbation, so the terms may be dropped. In the fourth term we have from equation (12) and the equations of motion (16)

$$\frac{1}{p_0}\frac{dp_0}{dt} = -\frac{1}{a}\frac{da}{dt} + \tfrac{1}{2}\frac{\partial h_{a\beta}}{\partial t}\gamma_a\gamma_\beta . \tag{24}$$

On multiplying equation (22) by p_0^3, integrating over p_0, and using equations (16), (19), (20), (24), and the equation

$$\frac{d\mathcal{E}}{dt} = -\frac{4\mathcal{E}}{a}\frac{da}{dt} , \tag{25}$$

we obtain the first-order equation

$$\frac{\partial\delta}{\partial t} + \frac{\gamma_a}{a}\frac{\partial\delta}{\partial x^a} - 2\gamma_a\gamma_\beta\frac{\partial h_{a\beta}}{\partial t} = \sigma n_e\left(\frac{4\pi}{\mathcal{E}}\int f_+ p_0^3 dp_0 - \delta - 1\right) . \tag{26}$$

We assume that the scattered radiation is isotropic in the matter rest frame. Since the distribution function is an invariant,

$$f_+(p_0, \gamma) = f'_+[p'_0(p_0, \gamma)] = \int f'(p'_0, \gamma')d\Omega'/4\pi , \tag{27}$$

where the primes refer to the locally Minkowski matter rest frame. With equations (23) and (27), the first term in the parentheses on the right-hand side of equation (26) becomes

$$\int f'd\Omega'p_0^3 dp_0/\mathcal{E} = (1 + 4\gamma_a v^a)\int f'p'_0 d^4p'/\mathcal{E} . \tag{28}$$

The integral on the right side of this equation is the radiation-energy density, and this is given by equation (21a) to terms of first order. With this result equation (26) finally becomes

$$\frac{\partial \delta}{\partial t} + \frac{\gamma_a}{a} \frac{\partial \delta}{\partial x^a} - 2\gamma_a \gamma_\beta \frac{\partial h_{a\beta}}{\partial t} = \sigma n_e (\delta_r + 4\gamma_a v^a - \delta) . \tag{29}$$

d) Description of the Matter

The matter is supposed to be an ideal fluid, with mass density

$$\rho_m(x, t) = \rho(t)[1 + \delta_m(x, t)] , \tag{30}$$

where $\rho(t)$ is the unperturbed value. The stress-energy tensor is

$$(T_m)_{ij} = \rho_m u_{mi} u_{mj} . \tag{31}$$

The motion of the matter is determined by the equations

$$(T_m)^{ij}{}_{;j} = g^i , \tag{32}$$

where in the locally Minkowski matter rest frame

$$g^0 = 0 , \qquad g^a = \sigma n_e (T_r)^{0a} . \tag{33}$$

Here $(T_r)^{0a}$ is the radiation-energy flux in this coordinate system. The covariant generalization of equations (33) is

$$g^i = \sigma n_e [(T_r)^{ij} u_{mj} - u_m{}^i (T_r)^{ik} u_{mj} u_{mk}] . \tag{34}$$

Letting $v^a = a v_m{}^a$ be the proper matter velocity measured by an observer at rest in the time-orthogonal coordinate system, and using equations (21), (32), and (34), we obtain, to first order,

$$\frac{dv^a}{dt} + \frac{v^a}{a} \frac{da}{dt} = \frac{\sigma n_e \mathcal{E}}{\rho} \left(f_a - \tfrac{4}{3} v^a \right) , \tag{35a}$$

$$\frac{\partial \delta_m}{\partial t} = \tfrac{1}{2} \frac{\partial h}{\partial t} - \frac{v^a{}_{,a}}{a} , \qquad h = \Sigma h_{aa} . \tag{35b}$$

e) Plane-Wave Decomposition

Since the spatial coordinates x^a do not appear in the coefficients of the linear perturbation equations (29) and (35), we can decompose the perturbation into complex plane waves, for example,

$$\delta_m = \Sigma \delta(m; k) \exp (ik \cdot x) . \tag{36}$$

In writing the differential equations for a single plane-wave component we generally omit the index k, and we choose the coordinates such that the x^3 axis is along k. Then by symmetry $h_{11} = h_{22}$, and $h_{12} = h_{23} = h_{13} = 0$. (We ignore gravitational radiation.) For a single plane-wave component, equation (29) is

$$\frac{d\delta}{dt} + \frac{ik\mu\delta}{a} + \Phi = \sigma n_e (\delta_r + 4\mu v - \delta) , \qquad \mu \equiv \gamma_3 = \cos \theta ,$$

$$\Phi = (1 - 3\mu^2) \frac{dh_{33}}{dt} - (1 - \mu^2) \frac{dh}{dt} , \qquad h = 2h_{11} + h_{33} . \tag{37}$$

Equations (21b) and (35) are

$$\frac{dv}{dt} + \frac{v}{a} \frac{da}{dt} = \frac{\sigma n_e \mathcal{E}}{\rho} \left(f - \tfrac{4}{3} v \right) , \tag{38a}$$

$$\frac{d\delta_m}{dt} = \tfrac{1}{2}\frac{dh}{dt} - \frac{ikv}{a} , \tag{38b}$$

and

$$f = \tfrac{1}{2}\int_{-1}^{+1}\delta\mu d\mu . \tag{38c}$$

In these equations we have dropped the index $\alpha = 3$.

In vector k in equation (36) is expressed in comoving coordinates. In the graphs displayed below the unit of k is chosen such that the comoving wavelength $2\pi/k$ is expressed in units of 10^{25} cm/T at epoch T (° K). Associated with k is a characteristic time-independent mass defined to be the mass within a sphere with diameter equal to the wavelength,

$$\mathfrak{M}(k) = \tfrac{1}{6}\pi\rho_0\left(\frac{2\pi \times 10^{25} \text{ cm}}{kT_0}\right)^3 . \tag{39}$$

f) Gravitational Field Equations

In a plane-wave perturbation there are only two independent components to the perturbed metric. The field equations are obtained by substituting the metric into Einstein's equations or the scalar-tensor field equations, and using the matter and radiation stress-energy tensors (eqs. [21], [31]). For the general-relativity cosmologies we use the two field equations

$$\frac{d^2h}{dt^2} + \frac{2}{a}\frac{da}{dt}\frac{dh}{dt} = 8\pi G(\rho\delta_m + 2\mathcal{E}\delta_r) , \tag{40a}$$

$$\frac{dh_{33}}{dt} - \frac{dh}{dt} = -\frac{ia}{k}16\pi G(\mathcal{E}f + \rho v) . \tag{40b}$$

Equation (40a) is the 0–0 component of the field equations, and equation (40b) is the 0–3 component. The left-hand sides of these equations were first derived by Lifshitz (1946).

For the scalar-tensor cosmology equations (40) are generalized to

$$\frac{d^2h}{dt^2} + \frac{2}{a}\frac{da}{dt}\frac{dh}{dt} = \frac{8\pi G_0}{\lambda}\left[\frac{3 + 2\omega}{2 + \omega}\mathcal{E}(\delta_r - \psi) + \rho(\delta_m - \psi)\right]$$
$$+ \frac{4(1 + \omega)}{\lambda}\frac{d\psi}{dt}\frac{d\lambda}{dt} + 2\frac{d^2\psi}{dt^2} , \tag{41a}$$

$$\frac{dh_{33}}{dt} - \frac{dh}{dt} = -\frac{ia}{k}\frac{16\pi G_0}{\lambda}\frac{(3 + 2\omega)}{(4 + 2\omega)}(\mathcal{E}f + \rho v)$$
$$- 2(1 + \omega)\frac{\psi}{\lambda}\frac{d\lambda}{dt} - \frac{2d\psi}{dt} + \frac{2\psi}{a}\frac{da}{dt} , \tag{41b}$$

and the equation for the perturbation to the scalar field is

$$\frac{d^2\psi}{dt^2} + \frac{d\psi}{dt}\left(\frac{2}{\lambda}\frac{d\lambda}{dt} + \frac{3}{a}\frac{da}{dt}\right) + \psi\left(\frac{1}{\lambda}\frac{d^2\lambda}{dt^2} + \frac{3}{\lambda a}\frac{da}{dt}\frac{d\lambda}{dt} + \frac{k^2}{a^2}\right) - \frac{1}{2\lambda}\frac{dh}{dt}\frac{d\lambda}{dt}$$
$$= \frac{8\pi G_0}{(4 + 2\omega)\lambda}\rho\delta_m . \tag{41c}$$

The only difference between the general-relativity and scalar-tensor models is the gravitational field equations. Because we use the original Brans-Dicke (1961) formula-

tion, the description of matter and radiation (eqs. ([37] and [38]) is the same in the two theories.

III. APPROXIMATE SOLUTIONS

a) Solution to First Order in t_c

Equations (37), (38), and (40) or (41) determine the time variation of linear perturbations within the framework of our general assumptions. In principle, these equations can be integrated numerically from a given initial time, but this becomes impractical at very early epochs, when the mean free time $t_c = (\sigma n_e)^{-1}$ is very short. We employ instead the standard iterative approximation to the collision equation in powers of t_c, to obtain, in the limit of small t_c, approximate equations which are used at the start of the integration.

To zeroth order in t_c equation (37) says

$$\delta = \delta_r + 4\mu v . \tag{42}$$

On substituting this equation into the left side of equation (37) we obtain the first-order equation for δ which, when substituted back into the left-hand side of equation (37), yields the second-order equation,

$$\delta = \delta_r + 4\mu v - t_c \left[C - \frac{d}{dt}(Ct_c) - \frac{ik\mu}{a} t_c C \right] ,$$
$$C = \frac{d\delta_r}{dt} + 4\mu \frac{dv}{dt} + \frac{ik\mu\delta_r}{a} + \frac{4ik\mu^2 v}{a} + \Phi . \tag{43}$$

When this equation is integrated over μ, the left-hand side yields δ_r (eq. [21a]), so the quantity in brackets, integrated over μ, has to vanish. This result with equation (38b) yields the first of the desired equations,

$$\frac{d\delta_r}{dt} = \frac{4}{3}\frac{d\delta_m}{dt} - \frac{4}{3}Kt_c , \quad K = \frac{k^2\delta_r}{4a^2} - \frac{ik}{a}\frac{dv}{dt} . \tag{44}$$

Next we obtain an expression for f (eq. [21b]) by multiplying equation (43) by μ and integrating the result over μ. On using this expression in equation (38a), we find the equation of motion for the fluid,

$$(\rho + \tfrac{4}{3}\mathcal{E})\frac{dv}{dt} + \frac{\rho v}{a}\frac{da}{dt} = -\frac{1}{3}\frac{ik\delta_r\mathcal{E}}{a} - \frac{4}{3}\frac{\mathcal{E}}{ik}\frac{d}{dt}Kat_c$$
$$+ \frac{ikt_c\mathcal{E}}{a}\left[\frac{4}{5}\frac{ikv}{a} + \frac{d}{dt}(\tfrac{1}{3}\delta_r - \tfrac{4}{15}h_{33} - \tfrac{2}{15}h)\right] . \tag{45}$$

Next we use equation (38b) to eliminate the velocity from this equation and obtain the second of the desired equations,

$$(1 + R)\frac{d^2}{dt^2}(\delta_m - \tfrac{1}{2}h) + \frac{(1 + 2R)}{a}\frac{da}{dt}\frac{d}{dt}(\delta_m - \tfrac{1}{2}h)$$
$$= -\frac{k^2\delta_r}{4a^2} + \frac{1}{a}\frac{d}{dt}(at_cK) - \frac{k^2t_c}{5a^2}\frac{d}{dt}(\delta_r + h_{33} - h) , \tag{46}$$

where

$$R = 3\rho/4\mathcal{E} . \tag{47}$$

Finally, with equations (38b) and (45) we can reduce the second of equations (44) to the expression (valid to zeroth order in t_c)

$$K = \frac{R}{1 + R}\left[\frac{k^2\delta_r}{4a^2} + \frac{1}{a}\frac{da}{dt}\left(\frac{1}{2}\frac{dh}{dt} - \frac{d\delta_m}{dt}\right)\right] . \tag{48}$$

b) Limiting Solutions

We present solutions to equations (44), (46), and (40) or (41) in two limiting cases of interest.

i) $R = 0$, $t_c = 0$, and $a/k \gg t$

This limit applies to the very early Universe. The solutions are

$$\delta_m = \tfrac{3}{4}\delta_r \propto t^n , \qquad\qquad n = -1, \tfrac{1}{2}, 1 . \quad (49)$$

Different parts of these solutions have been previously obtained by Lifshitz (1946) and Hawking (1966). We use for initial values the most rapidly growing mode. For this mode, we have

$$\frac{d\delta_m}{dt} = \frac{\delta_m}{t} , \qquad \delta_r = \tfrac{4}{3}\delta_m , \qquad \frac{dh}{dt} = 2\frac{d\delta_m}{dt} . \quad (50)$$

Because in this solution the wavelength is greater than the horizon t, the reality of this density perturbation might be questioned. The point is that different parts of the Universe are evolving like independent Friedmann models, and different observers would find truly different variations of density with proper time. Equation (49) gives the fractional difference between the density histories seen by two observers separated by a distance greater than t.

In the scalar-tensor cosmology we have chosen initial values such that equation (8b) applies, which means that in the early radiation-dominated Universe λ approaches a constant. Also, in equation (41c) the source term for ψ is negligible in this limiting case, so we can choose the initial values

$$\psi = d\psi/dt = 0 , \quad (51)$$

and equations (49) and (50) still apply.

ii) $R \lesssim 1$, $a/k \ll t$

This limit applies to the regime (*b*) mentioned in § 1. Since the perturbation wavelength is much less than ct, the gravitational fields in equation (46) may be neglected. Then the adiabatic approximation to equations (44) and (46) is

$$\delta_m \propto [\exp \int (i\omega - \gamma)dt]/(1 + R)^{1/4} ,$$

$$\gamma = \frac{k^2 c^2 t_c}{6a^2(1 + R)^2} [R^2 + 0.8(R + 1)] , \qquad \omega = \frac{k}{a}[3(1 + R)]^{-1/2} , \qquad (52)$$

where we have assumed that the damping rate γ is much less than the frequency ω of the wave. The damping rate has been derived by Peebles (1967*a*) (in a circulated preprint, the value of γ is wrong because the viscosity of the radiation fluid was neglected) and by Field (1970*a*).

c) Joining Conditions

In the transition from numerical integration of the first-order equations (44) and (46) to the numerical integration of the collision equation we need starting values for the velocity and the radiation distribution function. These are fixed in terms of the variables in the first-order integration by equations (38b) and (43). In the second of these equations we use equation (45) to eliminate the rate of change of velocity. The resulting initial values are

$$v = \frac{ia}{k}\frac{d}{dt}(\delta_m - \tfrac{1}{2}h) ,$$

$$\delta(\mu) = \delta_r + 4\mu v - t_c\left[(1 - 3\mu^2)\frac{d}{dt}(\tfrac{4}{3}\delta_m + h_{33} - h) + \frac{4ia}{k}\mu K \right] . \qquad (53)$$

IV. RESIDUAL PERTURBATION TO THE MICROWAVE BACKGROUND

Following recombination of the primeval plasma, the initially adiabatic perturbation leaves a residual irregularity in the radiation field. This irregularity persists if the radiation is not subsequently scattered by intergalactic matter or by the matter in young galaxies, and it is our purpose here to give an expression for the expected effect in terms of observations of the microwave background. We consider here fluctuations on a small angular scale, of the order of 1° or less.

a) Time Dependence of the Radiation Perturbation

At some time t_f well after the period of recombination, we can assume that

$$\lambda_f = 2\pi a_f/k \ll t_f \ll t_c(t_f) , \qquad \rho \gg \varepsilon . \tag{54}$$

In this limit the gravitational field equations (40b) or (41b, c) reduce to

$$\frac{dh_{33}}{dt} = \frac{dh}{dt} , \tag{55}$$

and equation (37) becomes

$$\frac{d\delta}{dt} + \frac{ik\mu\delta}{a} = 2\mu^2 \frac{dh}{dt} . \tag{56}$$

To solve this equation we introduce the substitution

$$\delta = \bar{\delta} - \frac{2ia\mu}{k}\frac{dh}{dt} + \frac{2a}{k^2}\frac{d}{dt}\left(a\frac{dh}{dt}\right) . \tag{57}$$

With this change of functions equation (56) becomes

$$\frac{d\bar{\delta}}{dt} + \frac{ik\mu}{a}\bar{\delta} = 0 , \tag{58}$$

where we have dropped terms of order $(\lambda_f/t_f)^3$. We have kept the equation valid to this order because the residual perturbation to δ_m and $t\,dh/dt$ is much larger than the residual perturbation to δ.

By equations (57) and (58) the fractional perturbation to the radiation brightness at time t_1 is

$$\delta(t_1) = \bar{\delta}_f \exp\left(-ik\mu\tau\right) ,$$

$$\bar{\delta}_f = \delta_f + \frac{2ia_f\mu}{k}\frac{dh_f}{dt} - \frac{2a_f}{k^2}\frac{d}{dt}\left(a\frac{dh}{dt}\right)_f, \qquad \tau = \int_{t_f}^{t_1}\frac{dt}{a(t)} . \tag{59}$$

In principle we should correct $\delta(t_1)$ for the peculiar motion of our chosen time-orthogonal coordinate system. However, this generates only a slowly varying term (proportional to μ) in the brightness, so we ignore it.

b) Observed Temperature Fluctuation

Equation (59) is based on the assumption that curvature may be neglected. In the late stages of expansion, at time $t > t_1$, spatial curvature becomes important. To obtain the fractional perturbation to the radiation brightness at the present time t_0, we trace back along the path of a light ray to the epoch t_1. At this epoch we set up a Cartesian coordinate system with (x, y)-axes perpendicular to the light ray. If we observe along a direction fixed by the two orthogonal angles (ψ_1, ψ_2) relative to the chosen light ray, the observed brightness is

$$\delta(t_0, \psi_1, \psi_2) = \Sigma\delta(k; t_1) \exp\left(ik\cdot x\right) , \tag{60}$$

where we are now summing over Fourier components (eq. [36]), k, and we have distinguished the individual amplitudes by k. We imagine that the observation scans only a small part of the sky, so that ψ_1, ψ_2 are small angles, and x has Cartesian components $(r\psi_1, r\psi_2, r)$, where r is the coordinate distance given by

$$r = R \sin \frac{1}{R} \int_{t_1}^{t_0} \frac{dt}{a(t)} \qquad \text{(closed)},$$

$$r = \int_{t_1}^{t_0} \frac{dt}{a(t)} \qquad \text{(flat)}, \qquad (61)$$

$$r = R \sinh \frac{1}{R} \int_{t_1}^{t_0} \frac{dt}{a(t)} \qquad \text{(open)},$$

for the different cosmological models (Landau and Lifshitz 1962). R is the coordinate radius of curvature (eq. [3]).

The brightness pattern (60) should be folded against the gain of the antenna. We assume that the gain is a Gaussian with resolving power $\Delta\psi$ independent of wavelength, so that the observed brightness is

$$\delta'_0(\psi'_1, \psi'_2) = \int \delta(t_0, \psi_1, \psi_2) F(\psi_1 - \psi'_1, \psi_2 - \psi'_2) d\psi_1 d\psi_2,$$

$$F(\psi_1, \psi_2) = \frac{1}{2\pi(\Delta\psi)^2} \exp\left[-(\psi_1^2 + \psi_2^2)/2\Delta\psi^2\right]. \qquad (62)$$

Now we use equation (60) for δ in equation (62), and we find

$$\delta'_0(\psi_1, \psi_2) = \Sigma\delta(k) \exp\left[-ir(k_x\psi_1 + k_y\psi_2 - k_z) - \tfrac{1}{2}(k_x^2 + k_y^2)r^2\Delta\psi^2\right]. \qquad (63)$$

If the individual Fourier components are assumed to have randomly chosen phases, the observed mean square fractional deviation of the brightness from the mean is

$$\langle|\delta'_0|^2\rangle = \Sigma|\bar{\delta}_{kf}|^2 \exp\left[-(k_x^2 + k_y^2)r^2\Delta\psi^2\right]. \qquad (64)$$

As usual, we replace the sum by an integral,

$$\langle|\delta'_0|^2\rangle = \int_0^\infty G(k, \Delta\psi) dk,$$

$$G(k, \Delta\psi) = \frac{V}{(2\pi)^2} \int_{-1}^{+1} d\mu k^2 |\bar{\delta}_{kf}|^2 \exp\left[-k^2(1 - \mu^2)r^2\Delta\psi^2\right], \qquad (65)$$

where the Fourier wave is fixed to be periodic in the large volume V. The normalization of equation (65) is fixed by the assumed amplitude of the residual perturbation to the matter distribution (§ VI).

In all this computation we have been able to concentrate on the radiation brightness integrated over frequency. This reduction of variables makes the numerical integration feasible, but it means that we lose detailed information of the spectrum of the residual irregularities in the background radiation. We can note, however, that as we follow the path of a photon back in time we end up at a spot in the primeval plasma near local thermal equilibrium. Because the photon mean free path is approximately independent of wavelength, the background looks like a mixture of blackbody spectra with weight independent of wavelength. Thus the rms fluctuation in antenna temperature is related to the rms fluctuation in brightness by the equation

$$\frac{\delta T}{T} \approx \tfrac{1}{4}\langle|\delta'_0|^2\rangle^{1/2}. \qquad (66)$$

V. RESULTS OF THE INTEGRATION: SHORT-WAVELENGTH LIMIT

In this section we consider that part of the perturbation with wavelength at recombination $\ll ct$. In this limit the perturbation to the gravitational field is unimportant, so we can drop h and h_{33} from the collision equation (37).

In accordance with the philosophy expressed in § Ia, we start the integration in the regime (b), where the perturbation acts like an acoustic wave, and we assume that the phase of each acoustic mode is chosen at random. Then for each mode the quantity of interest is the amplitude

$$\delta_s = [\delta_m(1)^2 + \delta_m(2)^2]^{1/2} ; \tag{67}$$

where $\delta_m(1)$ and $\delta_m(2)$ differ in phase by $90°$.

In the numerical integration the initial values are fixed by the adiabatic solution (52), and the initial amplitude is chosen so that δ_s is unity in the very early Universe. Because
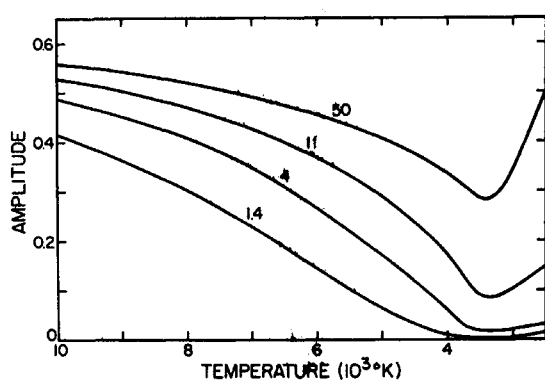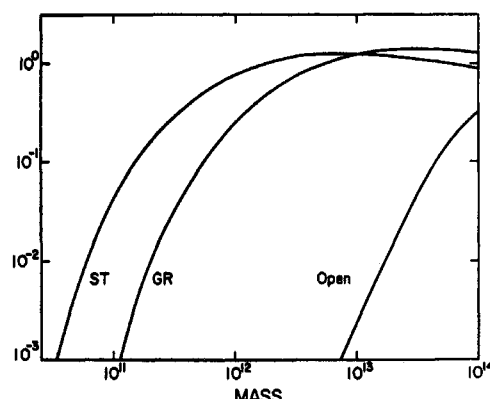

Fig. 2

Fig 3

Fig. 2.—Time variation of the amplitude δ_s (eq. [67]) of the perturbation to the matter density in the cosmologically flat general-relativity model. The parameter is the characteristic mass (eq. [39]) in units of $10^{11} \mathfrak{M}_\odot$.

Fig. 3.—Transfer function for an open general-relativity model $\rho_0 = 0.03\rho_c$, the cosmologically flat general-relativity model (GR), and the flat scalar-tensor model (ST). The amplitude is normalized to unity when $T \lesssim 10^5$ ° K; the independent variable is the mass (eq. [39]) in units of solar masses.

this is a linear calculation, one is of course free to adjust the shape of the initial power spectrum and to adjust thereby the final result. The first-order equations (44) and (46) are integrated ahead in time until it becomes feasible to switch over to the direct integration of equations (37) and (38). We find by trial that the results are insensitive to the switching time. At recombination ($T \sim 2500°$ K) the radiation drag force rather abruptly becomes unimportant. Thereafter the perturbation to the mass density varies as

$$\delta_m = A t^a + B/t , \tag{68}$$

where $a = \frac{2}{3}$ in the general-relativity models (Lifshitz 1946), and $a = (4 + 2\omega)/(4 + 3\omega)$ in the scalar-tensor model (Nariai 1969). This solution is used to carry the perturbation to the epoch $T = 2000°$ K.

For the cosmologically flat general-relativity model the amplitude δ_s is plotted as a function of time in Figure 2. Each curve belongs to a fixed comoving propagation vector k, and the parameter labeling the curves is the characteristic mass defined by equation (39). The sharp upturn of the curves at the right-hand side of the figure results from the residual matter velocity.

The amplitude δ_s at the final epoch $T = 2000°$ K is shown as a function of mass (eq. [39]) in Figure 3 for three cosmological models. These curves may be called the transfer functions for initially adiabatic perturbations with randomly distributed phase. The

transfer function is larger in the scalar-tensor model because the model expands faster, so the decoupling of matter and radiation is more sharp. The transfer function for the open model is smaller because near recombination the photon mean free path is longer, so the dissipation is greater.

We discuss the possible significance of these results after we deal with the part of the perturbation with longer wavelength.

VI. RESULTS OF THE INTEGRATION: LONG WAVELENGTH

The numerical integration starts at the epoch $T = 10^8$ ° K, where the Universe is radiation dominated, $R \leq 10^{-3}$ (eq. [47]). The initial values are fixed to the most rapidly growing mode (eqs. [50] and [51]). The first-order equations (44) and (46) are numerically integrated to the epoch $T = 10000°$ K, at which point we can, for the long wavelengths considered here, switch over to numerical integration of equations (37) and (38) along with the gravitational field equations. These equations are integrated to $T = 200°$ K.

We have several checks on the numerical accuracy of this scheme. The initial time variation is checked against the solution (50). When the integration reaches the regime (*b*), we can check against the solution (52). We verify that the equations to first order in t_c are a good approximation by shifting the transition to integration of the collision equation from the epoch $10000°$ to $7000°$ K. We verify that, in cases where the curvature may be neglected, the quantity $|\bar{\delta}_{kf}|^2$ (eqs. [59] and [65]) reaches a constant value by evaluating it at times earlier than $200°$ K.

a) Initial Conditions

Our assumptions fix the perturbation up to an initial amplitude for each wavelength. We choose for the initial power spectrum a sort of "cosmological white noise" spectrum indicated by the following argument.

The importance of a density perturbation in the early Universe is measured not only by the fractional density contrast $\delta\rho/\rho$ but also by the effect of the density contrast on the geometry—for any given $\delta\rho/\rho$ in the most rapidly growing mode one can always make the extent of the perturbation so large that it seriously affects the geometry, and even closes space back in on itself. A measure of the perturbation to the geometry due to a density perturbation with characteristic coordinate size r is the number

$$\epsilon = r/R_c , \tag{69}$$

where R_c is a coordinate measure of the local radius of curvature of space, and where in the radiation-dominated Universe the most rapidly growing mode for a density perturbation is (Peebles 1967*b*)

$$\delta_t = \delta\rho/\rho = 2t^2/a(t)^2 R_c^2 . \tag{70}$$

We choose the initial power spectrum of density irregularities such that ϵ is independent of the scale of length on which we examine the geometry. That is, we write the variance of the density as

$$\langle \delta_t^2 \rangle = \Sigma |\delta_{tk}|^2 \equiv \int \mathcal{P}(k) dk/k , \tag{71}$$

where

$$\mathcal{P}(k) \equiv V k^3 |\delta_{tk}|^2/2\pi^2 \tag{72}$$

is the contribution to the variance per logarithmic increment of the wavenumber k. This variance $\mathcal{P}(k)$ generates via equation (70) space curvature to the geometry observed on the coordinate length scale $r \sim k^{-1}$. Using equations (69) and (70), we write the initial power spectrum as

$$\mathcal{P}_i(k) = V k^3 |\delta_{tki}|^2/2\pi^2 \equiv 4(t_i\epsilon k/a_i)^4 . \tag{73}$$

Now we choose the shape of the initial power spectrum $|\delta_{tki}|^2$ such that the characteristic number ϵ in equation (73) is independent of k. Also, we will be considering amplitudes such that $\epsilon \ll 1$, so that the perturbation to the geometry is in a sense small.

This choice of initial power spectrum, $|\delta_{tki}|^2 \propto k$, has two interesting and perhaps attractive features. First, the initial perturbation contains no built-in characteristic lengths. The perturbation to the geometry looks the same on each scale of size. This would not have been the case if we had started with conventional white noise, $|\delta_{tki}|^2$ constant, because this does violence to the geometry at long wavelengths unless a long-wavelength cutoff is introduced. If the power spectrum varied as k^2, say, then we would have had the same problem at short wavelengths.

The second feature is that, with the initial value (73) in regime (*a*), in regime (*b*) the irregularity in the matter distribution is independent of length. To see this, note that
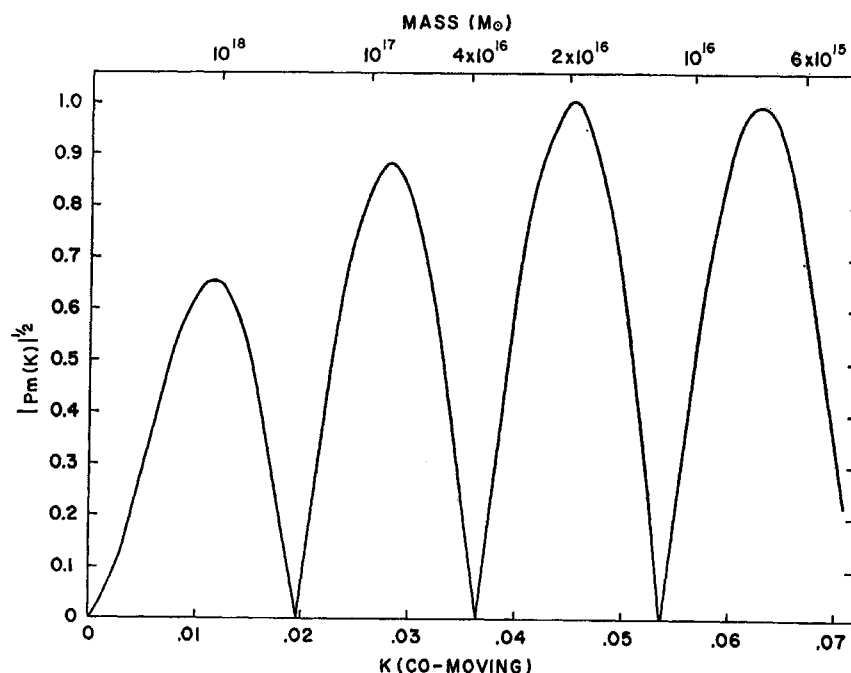

FIG. 4.—The residual mass-fluctuation spectrum $\mathcal{P}_m(k)^{1/2}$ (eq. [72]) in the open general-relativity model, $\rho_0 = 0.03\rho_c$ ($\rho_c = 1.8 \times 10^{-29}$ g cm^{-3}). The curve has been normalized to unity at maximum.

δ_{tk} grows in proportion to t until the proper wavelength $\lambda(t) = 2\pi a(t)/k$ becomes comparable to t. Because $a(t) \propto t^{1/2}$, we see that $|\delta_{tk}|^2$ grows by a total factor $\propto k^{-4}$, which cancels the factor k^4 in the right-hand side of equation (73), to make $\mathcal{P}(k)$ (eqs. [71] and [72]) independent of k.

The initial condition (73) determines the perturbation up to one normalizing factor (ϵ) which is fixed in the manner described below. We emphasize again that our numerical integration determines the transfer function in the framework of our assumptions, and it is quite a separate consideration that motivates the choice of starting values that seems reasonable to us. If different starting values seem more appropriate, they can of course be introduced by scaling the graphs presented below.

b) *Mass Density Fluctuation*

In Figures 4–7 we plot the mass-density-fluctuation spectrum well after recombination, as given by the function $\mathcal{P}_m(k)^{1/2}$, where

$$\mathcal{P}_m(k) = V k^3 |\delta_{m,k}|^2 / 2\pi^2 , \tag{74}$$

for the four cases of interest: the open, flat, and closed general-relativity models (cf. Figs. 4–7) and the flat scalar-tensor model. This is the contribution to the variance of the

mass density per logarithmic increment of k. In the figures the normalization is arbitrarily fixed to peak value unity.

c) Residual Irregularity in the Microwave Background

In Figure 8 we plot $G(k, \Delta\psi)$ (eq. [65]) for the cosmologically flat general-relativity model. The area under the curve for fixed $\Delta\psi$ gives the variance of the brightness of the observed background when the resolving power is $\Delta\psi$. Notice that $G(k, \Delta\psi)$ is appreciable only near the first peak of $\mathscr{P}_m(k)$. As $\Delta\psi$ decreases, the curve moves to the right because one is sensitive to shorter wavelength (larger wavenumber). The shift is not large, however, because the residual radiation perturbation at shorter wavelength is so very small. We conclude from Figure 8 that the experimental search for small-scale irregularities in the microwave background provides a test for the first big peak in Figure 5 (if the radiation has not suffered further scattering). The same conclusion holds for the other three cosmological models.
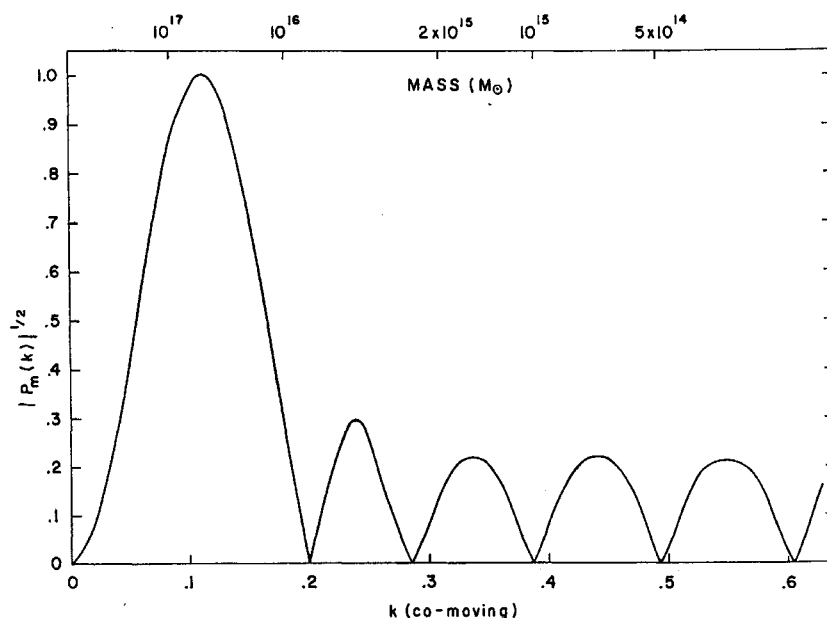

FIG. 5.—Same as Fig. 4 for the cosmologically flat general-relativity model, $\rho_0 = \rho_c$. The normalization is fixed to peak value unity.

In Figure 9 we plot the mean square fluctuation in the total brightness of the microwave background (eq. [65]; see also Table 1). In these curves the normalization has been fixed so that $\mathscr{P}_m(k)$ (Figs. 4–7) reaches the peak value unity at redshift $1 + Z_m = 10$. The time variation of the matter-density power spectrum is computed in the linear approximation, and our normalization means that at about redshift Z_m matter starts to fragment into separate and distinct bound systems with mass comparable to the mass function (eq. [39]) evaluated where $\mathscr{P}_m(k)$ is approaching unity. The observational limit shown on the figure is the upper limit estimated by Conklin and Bracewell after allowing for system noise. The results of the computation with this choice of Z_m are comparable to but smaller than this observational limit.

The above choice of Z_m may be too large. If Z_m were moved to a later epoch, it would reduce the required initial amplitude of the perturbation, hence reduce the mean square variation of the background. In Table 1 we list the factors by which the mean square variation of brightness must be multiplied when Z_m is reduced to smaller values (more recent epochs).
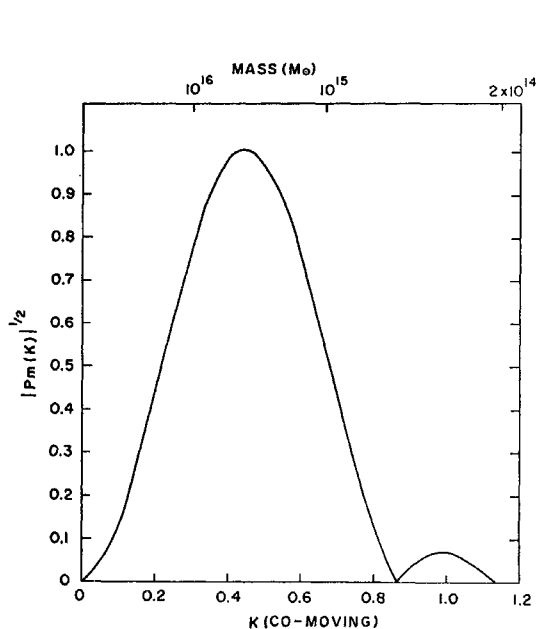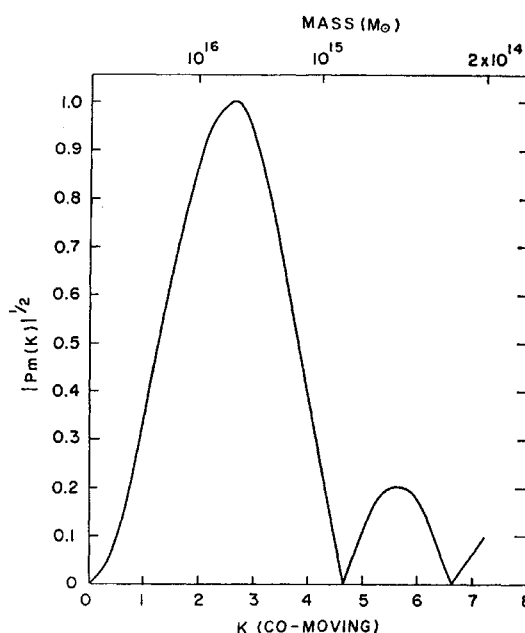
FIG. 6

FIG. 7

FIG. 6.—Same as Fig. 4 for the closed general-relativity model, $\rho_0 = 5\rho_c$.

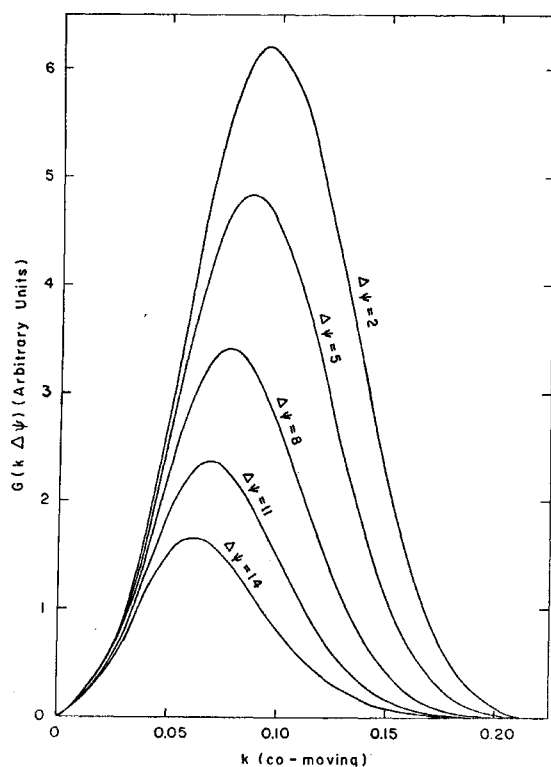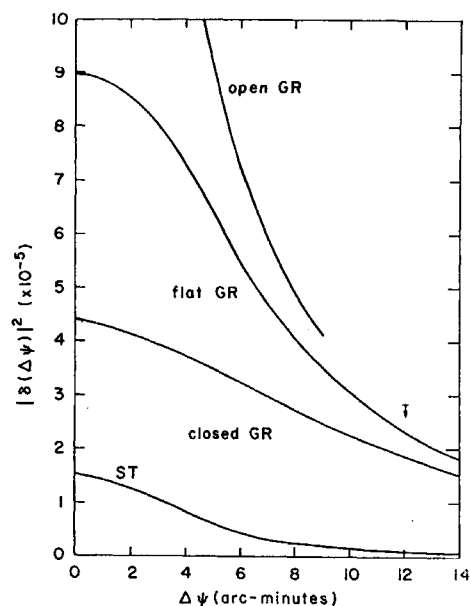FIG. 7.—Same as Fig. 4 for the flat scalar-tensor model ($\rho_0 = 1.24\rho_c$).

FIG. 8

FIG. 9

FIG. 8.—The function $G(k, \Delta\psi)$ determining the residual perturbation to the radiation as a function of angular resolution $\Delta\psi$ (eq. [65]). Unit of $\Delta\psi$ in the graph is minutes of arc. This curve applies to the cosmologically flat general-relativity model.

FIG. 9.—The mean square fluctuation of the observed bolometric brightness (eq. [65]) in the more dense cosmological models. The arrow is upper limit of Conklin and Bracewell (1967). The normalization is fixed so that $\mathcal{P}_m(k)$ reaches peak value unity at epoch $1 + Z_m = 10$.

We have shown no values for the expected fluctuations in the background in the open general-relativity model for angular resolution $\Delta\psi > 9'$. This is because the fluctuations are sensitive to very long wavelengths in this case, and our approximation of neglecting curvature no longer gives correct results.

VII. DISCUSSION

a) Comparison with Previous Results

It is of interest to compare the results of our numerical integration with the previous analytic estimates based on the assumption of a short photon mean free path for photons. Michie (1967) found that in a low-density model ($\rho_0 = 1 \times 10^{-30}$ g cm^{-3}), perturbations with characteristic mass $\leq 10^{11}$ $\mathfrak{M}_\odot$ are strongly damped before recombination, while a moderate amount of growth is achieved for $\mathfrak{M} \geq 10^{12}$ $\mathfrak{M}_\odot$. Silk (1968) estimated that perturbations are damped up to a mass of about 5×10^{11} $\mathfrak{M}_\odot$ in a low-density model ($\rho_0 = 1 \times 10^{-30}$ g cm^{-3}) and about 7×10^{10} $\mathfrak{M}_\odot$ in the flat model. We can define a characteristic mass for damping at the point where the transfer function falls to one-third

TABLE 1

RESIDUAL PERTURBATION $10^5 \times \langle|\delta'_0|^2\rangle^*$ TO THE MICROWAVE BACKGROUND

$\Delta\psi$†	Open General-Relativity Model	Flat General-Relativity Model	Closed General-Relativity Model	Flat Scalar-Tensor Model
0	73.0	9.0	4.40	1.55
3	16.0	7.8	4.00	1.09
6	7.4	5.4	3.20	0.44
9	4.1	3.5	2.45	0.22
12	...	2.3	1.80	0.13
15	...	1.6	1.30	0.084
$1+Z_m = 5$‡	0.61	0.25	0.23	0.20
$1+Z_m = 2$	0.41	0.040	0.026	0.023

* Equation (65).

† Angular resolution in minutes of arc if $1+Z_m = 10$, where the peak value of $\mathcal{P}_m$ at Z_m is unity.

‡ Correction factor to δ_0^2 when Z_m is reduced to the indicated values.

its maximum value. This characteristic mass is 10^{14} $\mathfrak{M}_\odot$ in the open model and 10^{12} $\mathfrak{M}_\odot$ in the flat model (Fig. 3). Both are significantly larger than the corresponding analytic estimates. This is to be expected because the analytic approximation is inadequate at recombination.

Field and Shepley (1968) found that when the characteristic mass of a perturbation is greater than 9×10^{15} $\mathfrak{M}_\odot$ in a flat general-relativity model, the amplitude grows continuously. This critical mass corresponds approximately to the first peak in Figure 5. Our value for the mass at this peak is $\mathfrak{M} \sim 5 \times 10^{16}$ $\mathfrak{M}_\odot$. These two characteristic masses are attributable to the same physical effect—the inability of pressure forces to stabilize the perturbation.

Residual perturbations to the microwave background have been computed by Longair and Sunyaev (1969). We find that the largest contribution to the residual perturbation comes from the first peak in the transfer function. For a mass $\mathfrak{M} \sim 5 \times 10^{16}$ $\mathfrak{M}_\odot$ (corresponding to the first peak in the flat general-relativity model), Longair and Sunyaev find angular scale $\sim 20'$, and fractional perturbation $\delta T/T \sim 2 \times 10^{-3}$ to the microwave-background temperature. Our result (Fig. 9) yields characteristic angular scale (width at half-maximum) $\sim 7'$, and $\delta T/T \sim 1.7 \times 10^{-3}$ at this angular resolution, in agreement with Longair and Sunyaev.

b) Possible Significance

It is well to bear in mind that in this calculation the initial density fluctuations are invoked in an ad hoc manner because we do not have a believable theory of how they may have originated. Also, it is entirely possible that we have left out some relevant force, possibly that provided by a primeval magnetic field. Our calculation thus is at best exploratory; but we have remarked that one might consider the results of the exploration encouraging if, for example, the characteristic numbers one derives correspond to known phenomena.

In the more dense cosmological models we tentatively identify two characteristic masses associated with the evolution of an initially adiabatic perturbation. The larger characteristic mass is on the order of the mass within the Hubble radius ct at recombination. One can understand this as follows: When the wavelength is very large, pressure gradients are negligible and the perturbation grows at a rate independent of wavelength. Because we started with an approximation to ordinary white noise (eq. [73]), the density variance increases with increasing wavenumber. This is a property of white noise, not of the Universe. The function $\mathcal{P}_m(k)$ stops increasing with increasing k when the perturbation wavelength becomes comparable to ct at recombination because the radiation pressure can slow or reverse the curve $\delta_m(t)$, leading to the oscillating behavior shown in Figures 4–7. In the open cosmological model (Fig. 4) the first peak is not very prominent, and it is hard to see how one could attach any special meaning to it. On the other hand, in the more dense models the first peak is a prominent feature.

The first characteristic feature might be identified with the great rich clusters of galaxies. Indeed, in the closed general-relativity model and in the flat scalar-tensor model the mass at the peak amounts to $\sim 5 \times 10^{15} \mathfrak{M}_\odot$, moderately close to some estimates of the mass of the Coma cluster, $\sim 1 \times 10^{15} \mathfrak{M}_\odot$. Unhappily the mass at the peak and even the existence of the peak as a prominent feature depend on the cosmological model. For example, in the flat general-relativity model the mass has shifted to $\sim 5 \times 10^{16} \mathfrak{M}_\odot$. Thus until the cosmological parameters are better established we can only claim the possibility that the theory can produce a prominent feature with mass which can be comparable to the mass of a great cluster of galaxies.

This possible interpretation has some attractive features. The rich clusters may be a remarkably uniform class of objects, which may call for a special mode of formation (Abell 1962). On the other hand, the mass within the Hubble radius at recombination surely is an interesting parameter of the cosmological model, and one would like to hope that the value of this number has some special significance for the nature of the Universe. The interesting point is that this number may be close to the typical mass of a great cluster of galaxies (Alpher, Herman, and Gamow 1967; Field 1970b).

The second characteristic mass comes from the rather sharp onset of linear dissipation with decreasing wavelength (again in the more dense models). In the linear approximation the power $\mathcal{P}_m(k)$ is an oscillating function of k (depending on the number of waves up to the epoch of recombination). With the chosen initial values this curve is about constant from peak to peak at longer wavelengths (Fig. 5). If nonlinear effects do not disturb the phase of the perturbation (Peebles 1970), then each curve in Figure 3 represents the envelope of the rapidly oscillating function $\mathcal{P}_m(k)^{1/2}$ at shorter wavelength. It is apparent from Figure 3 that in the more dense models there is a sharp cutoff at large wavenumber (short wavelength) associated with linear dissipation. Again, the characteristic mass at the cutoff depends on the cosmological model, so again we can only claim the possibility of an interesting coincidence of numbers: *if* the cosmological model is sufficiently dense, the characteristic mass defined by linear dissipation agrees with the mass of a big galaxy, $\sim 10^{11} \mathfrak{M}_\odot$.

In view of the enormous range of known masses of galaxies one might question whether it is reasonable to attach a single characteristic mass to the phenomenon. Although one

of us (P. J. E. P.) has in the past argued for the negative view, we are indebted to G. Abell for bringing the following suggestive point to our attention. In a rich cluster of galaxies the integrated galaxy luminosity function shows rather an abrupt change of slope at a characteristic absolute magnitude M^* (Abell 1962; Rood 1969). This means that the differential luminosity function has a local peak or plateau in the neighborhood of M^*. The brightest cluster member typically is a factor of 10 brighter than M^*. There are many more galaxies dimmer than M^* than there are galaxies brighter than M^*, but according to Abell's luminosity function the integrated luminosity of all the galaxies brighter than M^* is about equal to the total luminosity of all the dimmer members. If the mass-to-light ratio is about constant, the same remark applies to the integrated mass. The suggestion is then that when one counts on the basis of mass one may find that galaxies "typically" are large, with absolute magnitudes comparable to M^*.

The simple linear theory used here is not adequate to describe the fragmentation of the material into distinct bound systems. For this reason the mass estimates given here are only very rough approximations, and give no account of the expected dispersion of masses. Also, we can fix the time of fragmentation only in order of magnitude, as the epoch where the density contrast computed in the linear theory becomes comparable to unity.

If Figure 5 were taken literally, we would conclude that at about one single epoch, matter fragments into bound systems with masses ranging from $\sim 10^{11} \, \mathfrak{M}_\odot$ to $\sim 5 \times 10^{16} \, \mathfrak{M}_\odot$. That is, as the larger system starts to form out as a distinct cloud, it is itself fragmenting into smaller systems. This is not a capture hypothesis. Rather, it is supposed that galaxies and groups and clusters of galaxies form because there are initial irregularities on these scales. In this theory the order of formation is adjustable. It might be that protoclusters form first, and that galaxies fragment out during the initial collapse of the protocluster. With small adjustment of the initial power spectrum one can reverse this order without affecting the suggested interpretation of the two possibly characteristic masses.

For any choice of initial values it would be impossible to make small galaxies by the linear evolution of initially adiabatic perturbations (Peebles 1970). This is not necessarily a problem, however, for it is conceivable that a massive protogalaxy tends to fragment instead of collapsing to single system. There are also the initially isothermal perturbations. One interesting possibility is that the early Universe contains only adiabatic perturbations, but that the initial amplitude is large enough to cause nonlinear motions of matter and radiation prior to recombination. The result would be strong attenuation via shock waves. This attenuation must serve to smooth the radiation, but it could deposit the matter in an irregular fashion, producing an isothermal perturbation (Peebles 1970).

Finally, we discuss the expected irregularity of the microwave background on the assumption that this radiation has not been appreciably smoothed or perturbed by events after recombination. It will be recalled that this irregularity in the background is associated almost entirely with the first peak in the residual irregularity in matter density (Figs. 4–7). If this peak were identified with the great clusters of galaxies, we would have to fix the redshift at formation as $Z_m \gtrsim 1$. Then in the flat general-relativity cosmology the mean square fluctuation of antenna temperature at the beamwidth used by Conklin and Bracewell (1967) could be as small as 0.04 times the Conklin-Bracewell limit (Fig. 9 and Table 1). In the closed general-relativity model, which gives a somewhat more reasonable cluster mass, the mean square fluctuation could be 0.02 times this limit. In the flat scalar-tensor model the minimum mean square fluctuation would be reduced to 0.001 times this limit. If the angular resolution could be reduced to 1 minute of arc, the expected mean square fluctuation in antenna temperature would be increased by a factor of about 3 in the more dense general-relativity models and by a factor of about 10 in the scalar-tensor model.

If the observational accuracy could be improved by these factors, it would test the idea that the great clusters originated as initially adiabatic perturbations, although one must always bear in mind that the irregularities in the radiation background may have been smoothed or increased by subsequent processes (Dautcourt 1969; Longair and Sunyaev 1969).

In the open model the Conklin-Bracewell limit does seriously restrict the possible amplitude of adiabatic perturbations unless the radiation has been subsequently smoothed. On the other hand, in the computed spectrum of the density perturbations (Fig. 4) the first peak, which produces most of the irregularity, comes at a very large mass, $\sim 10^{18} \, \mathfrak{M}_\odot$. That is, it is already apparent that in this model our initial-value assumption (eq. [73]) is inadequate. This spectrum must be modified to reduce the power at very long wavelengths, for otherwise we would have produced bound systems on a mass scale much too big. If the first few peaks are thus de-emphasized, the residual perturbation to the microwave background is accordingly reduced. We conclude that in the open model we can find no ready interpretation of the observational limit on the irregularity in the microwave background because we cannot attach a possible observational interpretation to the first peak in the density-fluctuation curve (Fig. 5).

We have benefited from discussions with a number of people, including G. O. Abell, R. H. Dicke, E. Fackerell, G. B. Field, and K. S. Thorne. This work was done in part while one of us (P. J. E. P.) enjoyed the hospitality of W. A. Fowler at the California Institute of Technology. We would like to thank the referee for pointing out an error with reference to equation (64).

REFERENCES

Abell, G. O. 1962, *Problems of Extra-Galactic Research*, ed. G. C. McVittie (New York: Macmillan Co.), p. 213.
Alpher, R. A., Herman, R., and Gamow, G. 1967, *Proc. Nat. Acad. Sci.*, **58**, 2179.
Bardeen, J. 1968, *A.J.*, **73**, S164.
Brans, C., and Dicke, R. H. 1961, *Phys. Rev.*, **124**, 925.
Conklin, E. K., and Bracewell, R. N. 1967, *Nature*, **216**, 777.
Dautcourt, G. 1969, *M.N.R.A.S.*, **144**, 255.
Dicke, R. H. 1968, *Ap. J.*, **152**, 1.
Field, G. B. 1970a, in preparation.
———. 1970b, in *Star and Stellar Systems*, Vol. IX (Chicago: University of Chicago Press) (in press).
Field, G. B., and Shepley, L. C. 1968, *Ap. and Space Sci.*, **1**, 309.
Gamow, G. 1948, *Phys. Rev.*, **74**, 505.
Hawking, S. W. 1966, *Ap. J.*, **145**, 544.
Landau, L. D., and Lifshitz, E. M. 1962, *The Classical Theory of Fields* (New York: Pergamon Press).
Lifshitz, E. M. 1946, *J. Phys. USSR*, **10**, 116.
Lindquist, R. W. 1966, *Ann. Phys.* (N.Y.), **37**, 487.
Longair, M. S., and Sunyaev, R. A. 1969, *Nature*, **223**, 719.
Michie, R. W. 1967, Kitt Peak National Observatory preprint.
Nariai, H. 1969, *Progr. Theoret. Phys.*, **42**, 544.
Peebles, P. J. E. 1965a, *Ap. J.*, **142**, 1317.
———. 1965b, *Lectures in Applied Mathematics*, **8**, *Relativity Theory and Astrophysics*, p. 274.
———. 1967a, in *Proceedings of the Texas Conference on Relativistic Astrophysics* (in press).
———. 1967b, *Ap. J.*, **147**, 859.
———. 1968, *ibid.*, **153**, 1.
———. 1969, *ibid.*, **157**, 1075.
———. 1970, *Phys. Rev., D*, **1**, 397.
Peebles, P. J. E., and Dicke, R. H. 1968, *Ap. J.*, **154**, 891
Rood, H. J. 1969, *Ap. J.*, **158**, 657.
Sachs, R. K., and Wolfe, A. M. 1967, *Ap. J.*, **147**, 73.
Silk, J. 1968, *Ap. J.*, **151**, 459.
Wolfe, A. M. 1969, *Ap. J.*, **156**, 803.
Zel'dovich, Ya. B. 1967, *Soviet Phys.—Usp.*, **9**, 602.